Criegee intermediate decomposition pathways for the formation of *o*-toluic acid and 2-methylphenylformate

Chaiyaporn Lakmuang,[1] Asja A. Kroeger,[2] and Amir Karton[2,*]

[1]Department of Chemistry, Faculty of Science, Mahidol University, Bangkok, Thailand

[2]School of Molecular Sciences, The University of Western Australia, Perth, WA 6009, Australia

ABSTRACT

We use Gaussian-4 theory to investigate the reaction mechanism for the conversion of a 2-methylstyrene-based Criegee intermediate into *o*-toluic acid and 2-methylphenylformate. *o*-Toluic acid can be formed via a α-hydroxyalkyl-hydroperoxide intermediate with an activation energy of $\Delta G^{\ddagger}_{298}$ = 82.9 kJ mol^{-1} for the rate-determining-step (RDS). The RDS for the formation of 2-methylphenylformate has an activation energy of $\Delta G^{\ddagger}_{298}$ = 61.9 kJ mol^{-1}. Formation of the *o*-toluic acid product is more exergonic by 67.4 kJ mol^{-1}. Consistent with recent experimental results, our high-level calculations show that *o*-toluic acid is the thermodynamic product and 2-methylphenylformate is the kinetic product.

Cite as:
C. Lakmuang, A. A. Kroeger, A. Karton, Chem. Phys. Lett. 748, 137399 (2020). https://doi.org/10.1016/j.cplett.2020.137399

*Corresponding author E-mail address: amir.karton@uwa.edu.au.

Introduction

Ozonolysis of unsaturated hydrocarbons is a dominant oxidation pathway in the troposphere leading to the formation of Criegee intermediates (CIs). CIs play a major role in the chemistry of the troposphere by producing secondary organic aerosols (SOAs)[1] which impact both air pollution and climate.[2,3,4] Recently, Chiappini *et al.*[5] used Fourier-transform infrared spectroscopy and gas chromatography-mass spectroscopy to investigate the ozonolysis of two atmospherically relevant anthropogenic aromatic alkenes: 2-methylstyrene and indene.[6,7,8] They found that in the case of 2-methylstyrene, ozone adds mainly on the exocyclic double bond yielding a 2-methylstyrene-based CI. The CI is then converted to *o*-toluic acid as a major product (140 ± 50 μg m^{-3}) and 2-methylphenylformate as a minor product (1.5 ± 0.4 μg m^{-3}). They suggested that this intramolecular conversion may proceed via a hypothetical dioxirane intermediate as shown in Figure 1.

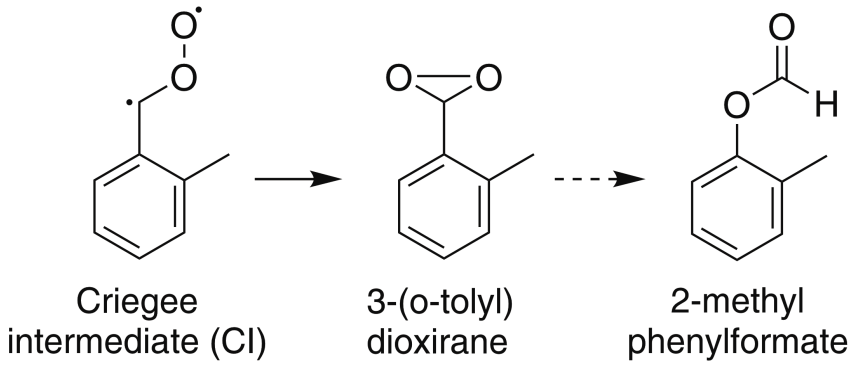

Figure 1. Formation of 2-methylphenylformate from a 2-methylstyrene-based Criegee intermediate via a hypothetical dioxirane intermediate proposed in ref. 5.

In the present work we use the high-level Gaussian-4 (G4) thermochemical protocol[9,10] to explore in detail the mechanisms for the intramolecular conversions of this 2-methylstyrene-based

CI into *o*-toluic acid (thermodynamic product) and 2-methylphenylformate (kinetic product). We find that *o*-toluic acid can be formed via two competing reaction pathways involving a hydroperoxide intermediate. Both channels involve a water molecule either as a catalyst or a reagent. Formation of the 2-methylphenylformate product proceeds via the hypothetical dioxirane intermediate proposed in ref. 5. We show here that both channels are accessible at room temperature, however, formation of 2-methylphenylformate is kinetically favored and formation of *o*-toluic acid is thermodynamically favored.

Computational details

High-level ab initio and density functional theory calculations were carried out using the Gaussian 09 program suite.[11] The Gaussian-4 (G4) theory is used for calculating Gibbs free potential energy surfaces for the conversion of the 2-methylstyrene-based CI to *o*-toluic acid and 2-methylphenylformate. G4 theory approximates the CCSD(T)/CBS energy (coupled cluster energy with single, double, and quasiperturbative triple excitations at the complete basis-set limit).[12,13] The computational protocol of G4 theory has been specified and rationalized in detail in refs. 9 and 10. It has been found to produce thermochemical and kinetic properties (such as reaction energies, bond dissociation energies, enthalpies of formation, and reaction barrier heights) with mean absolute deviations (MADs) from highly accurate experimental/theoretical data below the threshold of chemical accuracy (i.e., with MADs below 1 kcal mol^{-1}).[9,10,14,15,16,17,18,19,20] Importantly, G4 theory has also been recently found to provide good performance for reaction energies and barrier heights for ring-closing reactions involving atmospherically important Criegee intermediates.[21] We also note that the $\mathcal{T}_1$ diagnostics[22,23] for the CIs (and associated TSs and reaction intermediates) considered in the present work range between 0.01–0.03 (Table S1 of the

Supporting Information). These values indicate that these systems exhibit mild-to-moderate multireference character and that the CCSD(T)/CBS level of theory should be adequate for treating the CIs considered in the present work.

The geometries and harmonic vibrational frequencies were obtained at the B3LYP/6-31G(2df,p) level of theory as prescribed in the G4 protocol.[24,25,26,27] Zero-point vibrational energy (ZPVE), thermal enthalpy ($H_{298}–H_0$), and entropy (S) corrections were obtained from these frequencies within the rigid rotor-harmonic oscillator approximation. The main text reports Gibbs free energy (ΔG_{298}) reaction profiles, whilst reaction profiles on the electronic (ΔE_e), enthalpic at 0 K (ΔH_0), and enthalpic at 298 K (ΔH_{298}) potential energy surfaces are provided as Supporting information (Table S2). The equilibrium structures were verified to have all real harmonic frequencies, and the transition structures to have only one imaginary frequency. The connectivities of the transition structures were confirmed by performing intrinsic reaction coordinate (IRC) calculations.[28,29]

Results and Discussion

Figure 2 shows the Gibbs free potential energy surfaces (PESs) at 298 K for the conversion of the CI to *o*-toluic acid (pathways A and B) and 2-methylphenylformate (pathway C). The structures of the reactants, reaction intermediates, transition structures, and products located along the reaction profiles are shown in Figure 3. It is well established that Criegee intermediates have a singlet ground state, with the lowest lying triplet state typically located over 100 kJ mol^{-1} above the ground state. For example, the singlet-triplet gap in the prototypical Criegee intermediate (H_2COO) was calculated to be 128.4 (at the CCSD(T)/cc-pVTZ level of theory)[30] and 126.8 (using the CBS-QB3[31] composite method)[32] kJ mol^{-1}. Before proceeding to a detailed discussion of these

reaction pathways, it is of interest to see by how much the presence of an aromatic substituent in the 2-methylstyrene-based Criegee intermediate affects the singlet-triplet gap. At the G4 level we obtain a singlet-triplet gap of 116.9 kJ mol^{-1} for this system on the Gibbs free potential energy surface at 298 K. This energy gap is well above the Gibbs free barrier heights for the rate-determining steps in pathway A (82.9), water-catalyzed pathway B (95.0), and pathway C (61.9 kJ mol^{-1}) (*vide infra*) and therefore the triplet PES is not further considered in this work.

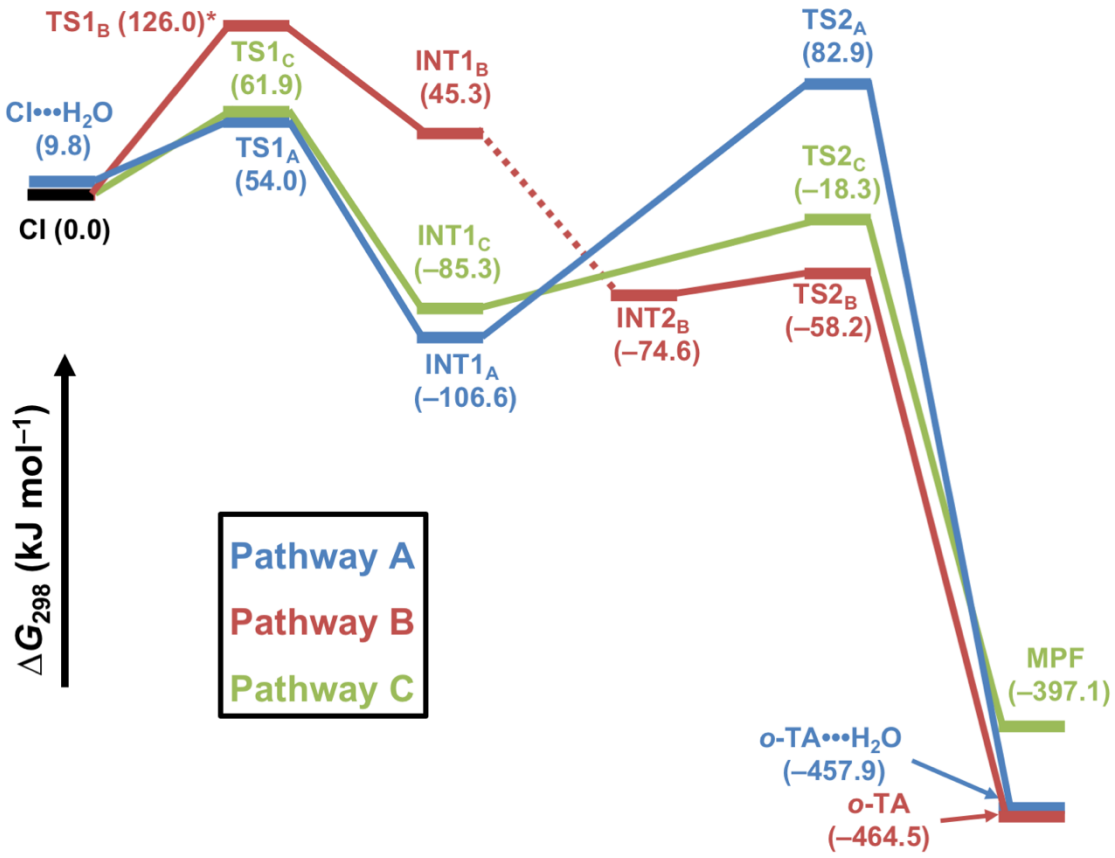

Figure 2. Gibbs-free energy surfaces at 298 K (G4 theory, kJ mol^{-1}) for the intramolecular conversion of the 2-methylstyrene-based CI to *o*-toluic acid (*o*-TA) (pathways A and B) and 2-methylphenylformate (MPF) (pathway C). *Note that the Gibbs free energy barrier for TS1B is reduced from 126.0 to 95.0 kJ mol^{-1} upon catalysis by a single water molecule (see text).

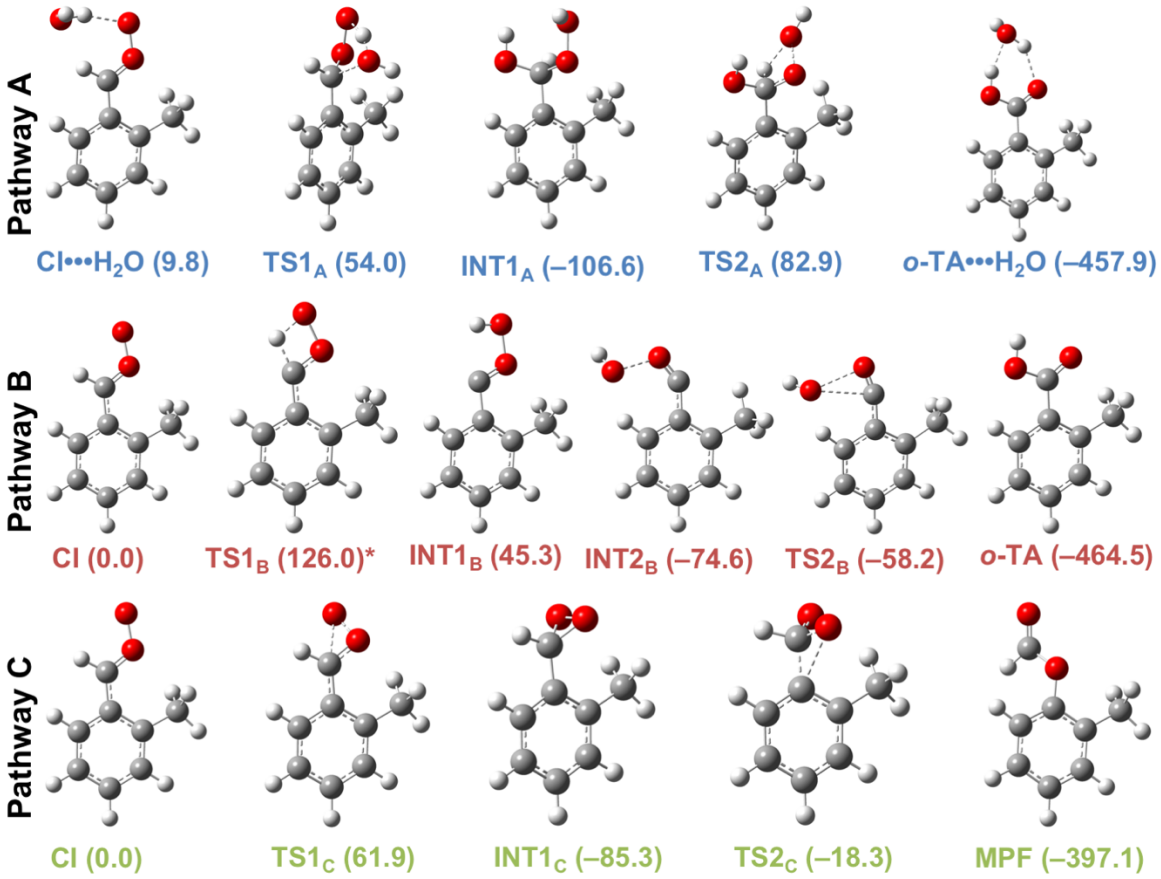

Figure 3. Optimized structures of the Criegee intermediate (CI) reactant, reaction intermediates, transition structures (TSs), and *o*-toluic acid (*o*-TA) and 2-methylphenylformate (MPF) products located along the reaction profiles for the intramolecular conversion of the 2-methylstyrene-based CI to *o*-toluic acid (pathways A and B) and 2-methylphenylformate (pathway C). Gibbs free energies (in kJ mol^{-1}) relative to CI and H_2O (pathway A) and relative to CI (pathways B and C) are given in parenthesis (see also Figure 2 for a schematic representation of the PESs). Atomic color scheme: H, white; C, gray; O, red. *Note that the Gibbs free energy barrier for $TS1_B$ is reduced from 126.0 to 95.0 kJ mol^{-1} upon catalysis by a single water molecule (see text).

Formation of *o*-toluic acid via α-hydroxyalkyl-hydroperoxide intermediate (pathway A). We begin by examining the formation of *o*-toluic acid via the commonly invoked α-hydroxyalkyl-hydroperoxide intermediate.[33,34,35,36,37] This reaction pathway involves a water molecule and proceeds via formation of a CI•••H_2O complex (Figure 3). The formation of this complex is exothermic by 27.3 kJ mol^{-1} on the enthalpic PES (ΔH_{298}, G4 theory). However, due to entropic effects, it is endergonic by 9.8 kJ mol^{-1} on the Gibbs free energy surface (ΔG_{298}, Figure 2). This complexation is followed by addition of the water molecule to the CI leading to the formation of a stable α-hydroxy hydroperoxide intermediate (INT1$_A$, Figures 2 and 3). This step is associated with a low reaction barrier height of $\Delta G^{\ddagger}_{298}$ = 54.0 kJ mol^{-1}. The α-hydroxy hydroperoxide intermediate lies 106.6 kJ mol^{-1} below the energy of the free reactants and is the most stable reaction intermediate considered in the present work.

Next, the hydroxyl of the hydroperoxide group can abstract the hydrogen from the alpha carbon leading to the formation of *o*-toluic acid and regeneration of a water molecule. The reaction barrier height for this step is relatively large ($\Delta G^{\ddagger}_{298}$ = 82.9 kJ mol^{-1}, Figure 2) since the TS involves a four-membered ring formed between the carbon, hydrogen, and two hydroperoxide oxygens (TS2$_A$, Figure 3). Inspection of the bond angles in TS2$_A$ relative to those in INT1$_A$ reveals that the four-membered ring in the TS is strained. For example, ∠COO = 89.7° (TS2$_A$) and 105.7° (INT1$_A$) and ∠OCH = 95.2° (TS2$_A$) and 107.0° (INT1$_A$). We note that since this reaction pathway already involves one water molecule, due to entropic effects inclusion of a second water molecule does not reduce the free energy barrier height and results in $\Delta G^{\ddagger}_{298}$ = 86.4 kJ mol^{-1}.

Finally, we note that, similar to the initial CI•••H_2O complex, formation of the hydrogen bond in the resulting *o*-toluic acid•••H_2O complex is exothermic by 33.5 kJ mol^{-1} on the enthalpic PES (ΔH_{298}, G4 theory), but endergonic by 6.7 kJ mol^{-1} on the Gibbs free energy surface (ΔG_{298},

Figure 2). Thus, in the gas-phase this complex will not form and the overall reaction energy for the formation of free *o*-toluic acid is $\Delta G^{\ddagger}_{298}$ = –464.5 kJ mol^{-1} (Figure 2) providing a strong thermodynamic drive for this reaction pathway.

Formation of *o*-toluic acid via vinyl hydroperoxide intermediate (pathway B). Let us turn our attention to the alternative route for the formation of *o*-toluic acid via a different hydroperoxide intermediate. This reaction pathway proceeds via a intramolecular 1,3-proton transfer to form the well-known hydroperoxide intermediate.[38,39,40,41] This step is the rate-determining step (RDS) for this pathway with $\Delta G^{\ddagger}_{298}$ = 126.0 kJ mol^{-1}. The large reaction barrier height may be attributed to the strain energy in the four-membered-ring TS for the proton transfer (TS_{1B}, Figure 3). Inspection of the bond angles in $TS1_B$ relative to those in the reactant CI reveals that the four-membered ring in the TS is highly strained. For example, ∠COO = 100.5° ($TS1_B$) and 117.8° (CI) and ∠OCH = 80.2° ($TS1_B$) and 115.2° (CI). It has been previously found that a single water catalyst can stabilize similar cyclic proton-transfer TSs by converting a strained four-membered ring TS into a less strained six membered-ring TS.[40,42,43,44,45,46,47] In the present case, a single water catalyst reduces the reaction barrier height from 126.0 to 95.0 kJ mol^{-1} relative to the free reactants. The resulting hydroperoxide intermediate (INT_{1B}) lies 45.3 kJ mol^{-1} above the energy of the CI (Figure 2). In this unstable intermediate the O–O bond length is 1.505 Å and the peroxy hydrogen is *syn* to the toluene group. INT_{1B} can rearrange to a more stable intermediate (INT_{2B}) in which the peroxy hydrogen is *anti* to the toluene group with a much longer O•••O bond distance of 1.928 Å. We note that in INT_{2B} both the Ph–COOH and PhC=OOH bonds are shorter than in INT_{1B}, which could partly explain the greater stability of this intermediate. Namely, the Ph–COOH bond length is

1.472 (INT_{1B}) and 1.433 (INT_{2B}) Å; and the PhC=OOH bond length is 1.266 (INT_{1B}) and 1.168 (INT_{2B}) Å.

Finally, an additional intramolecular rearrangement, in which the loosely bound hydroxyl oxygen attacks the carbonyl carbon, leads to the formation of *o*-toluic acid (*o*-TA, Figures 2 and 3), which lies 464.5 kJ mol^{-1} below the CI reactant. The transition structure for this rearrangement (TS_{2B}, Figures 2 and 3) lies 58.2 kJ mol^{-1} below the CI reactant.

Formation of 2-methylphenylformate via a dioxirane intermediate (pathway C). The formation of the minor product 2-methylphenylformate from the 2-methylstyrene-based CI could proceed via the 3-(*o*-tolyl)dioxirane intermediate proposed in ref. 5 ($INT1_C$), see also discussion in refs. 33 and 48. This intramolecular reaction pathway (pathway C, Figures 2 and 3) proceeds via a ring-closing reaction to give 3-(*o*-tolyl)dioxirane which lies 85.3 kJ mol^{-1} below the CI ($INT1_C$). This step is the RDS for this pathway with $\Delta G^{\ddagger}_{298}$ = 61.9 kJ mol^{-1} ($TS1_C$). The dioxirane intermediate can undergo an intramolecular rearrangement in which one of the oxygens is inserted into the adjacent C–Ph bond to form the minor 2-methylphenylformate product which lies 397.1 kJ mol^{-1} below the CI reactant. This transition structure lies 18.3 kJ mol^{-1} below the CI reactant ($TS2_C$).

Conclusions

In summary, we use the G4 procedure to investigate the intramolecular conversion of a 2-methylstyrene-based CI to *o*-toluic acid and 2-methylphenylformate. We find that there are two reaction pathways for the formation of *o*-toluic acid – both proceed via hydroperoxide intermediates. Pathway A involves an addition of water to the CI to form α-hydroxyalkyl-

hydroperoxide followed by intramolecular hydrogen abstraction and regeneration of the water molecule. The second step is the RDS with $\Delta G^{\ddagger}_{298}$ = 82.9 kJ mol^{-1}. Pathway B starts with an intramolecular 1,3-proton transfer to form a hydroperoxide intermediate. This step is the RDS with $\Delta G^{\ddagger}_{298}$ = 126.0 kJ mol^{-1}, however, a water catalyst reduces the barrier to $\Delta G^{\ddagger}_{298}$ = 95.0 kJ mol^{-1}. Thus, overall pathway A is kinetically favorable by 12.1 kJ mol^{-1} over pathway B and is accessible at room temperature.

The pathway for the formation of 2-methylphenylformate (pathway C) proceeds via a dioxirane intermediate, the formation of which constitutes the RDS for the entire pathway with $\Delta G^{\ddagger}_{298}$ = 61.9 kJ mol^{-1}. Thus, this is the kinetically favorable pathway, however, it leads to the thermodynamically less stable product in accord with the Bell–Evans–Polanyi principle. These results are consistent with recent experimental results which show that *o*-toluic acid is the major product of the entire process.[5]

Supplementary data

$\mathcal{T}_1$ diagnostics for the CIs and associated transition structures and reaction intermediate considered in the present work (Table S1); reaction profiles on the electronic (ΔE_e), enthalpic at 0 K (ΔH_0), and enthalpic at 298 K (ΔH_{298}) potential energy surfaces (Table S2); and Cartesian coordinates for all the species considered in the present work (Table S3).

Acknowledgments

This research was undertaken with the assistance of resources from the National Computational Infrastructure (NCI), which is supported by the Australian Government. We gratefully acknowledge the provision of a Forrest Research Foundation Scholarship and an Australian

Government Research Training Program Stipend (to A.A.K.) and an Australian Research Council (ARC) Future Fellowship (to A.K., Project No. FT170100373).

References

[1] R. J. Griffin, D. R. Cocker III, J. H. Seinfeld, D. Dabdub, Estimate of global atmospheric organic aerosol from oxidation of biogenic hydrocarbons, *Geophys. Res. Lett.* 26 (1999) 2721–2724.

[2] D. Johnson, G. Marston, The gas-phase ozonolysis of unsaturated volatile organic compounds in the troposphere, *Chem. Soc. Rev.* 37 (2008) 699–716.

[3] M. Hallquist, J. C. Wenger, U. Baltensperger, Y. Rudich, D. Simpson, M. Claeys, J. Dommen, N. M. Donahue, C. George, A. H. Goldstein, J. F. Hamilton, H. Herrmann, T. Hoffmann, Y. Iinuma, M. Jang, M. E. Jenkin, J. L. Jimenez, A. Kiendler-Scharr, W. Maenhaut, G. McFiggans, T. F. Mentel, A. Monod, A. S. H. Prevot, J. H. Seinfeld, J. D. Surratt, R. Szmigielski, J. Wildt, The formation, properties and impact of secondary organic aerosol: current and emerging issues, *Atmos. Chem. Phys.* 9 (2009) 5155–5236.

[4] H. O. T. Pye, A. W. H. Chan, M. P. Barkley, J. H. Seinfeld, Global modeling of organic aerosol: the importance of reactive nitrogen (NO_x and NO_3), *Atmos. Chem. Phys.* 10 (2010) 11261–11276.

[5] L. Chiappini, E. Perraudin, N. Maurin, B. Picquet-Varrault, W. Zheng, N. Marchand, B. Temime-Roussel, A. Monod, A. Le Person, F. Bernard, G. Eyglunent, A. Mellouki, J.-F. Doussin, Secondary organic aerosol formation from aromatic alkene ozonolysis: influence of the precursor structure on yield, chemical composition, and mechanism, *J. Phys. Chem. A* 123 (2019) 1469–1484.

[6] N. Yassaa, B. Y. Meklati, E. Brancaleoni, M. Frattoni, P. Ciccioli, Polar and Non-Polar Volatile Organic Compounds (VOCs) in Urban Algiers and Saharian Sites of Algeria, *Atmos. Environ.* 35 (2001) 787–801.

[7] N. Schiavon, G. Chiavari, D. Fabbri, Soiling of Limestone in an Urban Environment Characterized by Heavy Vehicular Exhaust Emissions, *Environ. Geol.* 46 (2004) 448–455.

[8] D. R. Gentner, D. R. Worton, G. Isaacman, L. C. Davis, T. R. Dallmann, E. C. Wood, S. C. Herndon, A. H. Goldstein, R. A. Harley, Chemical Composition of Gas-Phase Organic Carbon Emissions from Motor Vehicles and Implications for Ozone Production, *Environ. Sci. Technol.* 47 (2013) 11837–11848.

[9] L. A. Curtiss, P. C. Redfern, K. Raghavachari, Gaussian-4 theory, *J. Chem. Phys.* 127 (2007) 124105.

[10] L. A. Curtiss, P. C. Redfern, K. Raghavachari, Gn Theory, *WIREs Comput. Mol. Sci.* 1 (2011) 810–825.

[11] M. J. Frisch, G. W. Trucks, H. B. Schlegel, G. E. Scuseria, M. A. Robb, J. R. Cheeseman, G. Scalmani, V. Barone, B. Mennucci, G. A. Petersson, H. Nakatsuji, M. Caricato, X. Li, H. P. Hratchian, A. F. Izmaylov, J. Bloino, G. Zheng, J. L. Sonnenberg, M. Hada, M. Ehara, K. Toyota, R. Fukuda, J. Hasegawa, M. Ishida, T. Nakajima, Y. Honda, O. Kitao, H. Nakai, T. Vreven, J. A. Montgomery, Jr., J. E. Peralta, F. Ogliaro, M. Bearpark, J. J. Heyd, E. Brothers, K. N. Kudin, V. N. Staroverov, R. Kobayashi, J. Normand, K. Raghavachari, A. Rendell, J. C. Burant, S. S. Iyengar, J. Tomasi, M. Cossi, N. Rega, J. M. Millam, M. Klene, J. E. Knox, J. B. Cross, V. Bakken, C. Adamo, J. Jaramillo, R. Gomperts, R. E. Stratmann, O. Yazyev, A. J. Austin, R. Cammi, C. Pomelli, J. W. Ochterski, R. L. Martin, K. Morokuma, V. G. Zakrzewski, G. A. Voth, P. Salvador, J. J. Dannenberg, S. Dapprich, A. D. Daniels, Ö. Farkas, J. B.

Foresman, J. V. Ortiz, J. Cioslowski, and D. J. Fox, Gaussian 09 (Gaussian, Inc., Wallingford CT, 2009).

[12] G. D. Purvis, R. J. Bartlett, A Full Coupled-Cluster Singles and Doubles Model: The Inclusion of Disconnected Triples. *J. Chem. Phys.* 1982, 76, 1910–1918.

[13] K. Raghavachari, G. W. Trucks, J. A. Pople, M. Head-Gordon, A Fifth-Order Perturbation Comparison of Electron Correlation Theories, *Chem. Phys. Lett.* 157 (1989) 479–483.

[14] A. Karton, N. Sylvetsky, J. M. L. Martin, W4-17: A diverse and high-confidence dataset of atomization energies for benchmarking high-level electronic structure methods, *J. Comput. Chem.* 38 (2017) 2063–2075.

[15] A. Karton, P. R. Schreiner, J. M. L. Martin, Heats of formation of platonic hydrocarbon cages by means of high-level thermochemical procedures, *J. Comput. Chem.* 37 (2016) 49–58.

[16] A. Karton, L. Goerigk, Accurate reaction barrier heights of pericyclic reactions: surprisingly large deviations for the CBS-QB3 composite method and their consequences in DFT benchmark studies, *J. Comput. Chem.* 36 (2015) 622–632.

[17] L.-J. Yu, F. Sarrami, R. J. O'Reilly, A. Karton, Reaction barrier heights for cycloreversion of heterocyclic rings: An Achilles' heel for DFT and standard ab initio procedures, *Chem. Phys.* 458 (2015) 1–8.

[18] L.-J. Yu, A. Karton, Assessment of theoretical procedures for a diverse set of isomerization reactions involving double-bond migration in conjugated dienes, *Chem. Phys.* 441 (2014) 166–177.

[19] A. Karton, J. M. L. Martin, Explicitly correlated benchmark calculations on C_8H_8 isomer energy separations: How accurate are DFT, double-hybrid and composite ab initio procedures? *Mol. Phys.* 110 (2012) 2477–2491.

[20] L. A. Curtiss, P. C. Redfern, K. Raghavachari, Assessment of Gaussian-4 theory for energy barriers, *Chem. Phys. Lett.* 499 (2010) 168–172.

[21] C. D. Smith, A. Karton, Kinetics and Thermodynamics of Reactions Involving Criegee Intermediates: An Assessment of Density Functional Theory and Ab Initio Methods Through Comparison with CCSDT(Q)/CBS Data, *J. Comput. Chem.* 41 (2020) 328–339.

[22] T. J. Lee, P. R. Taylor, A diagnostic for determining the quality of single-reference electron correlation methods, *Int. J. Quantum Chem. Symp.* 23 (1989) 199–207.

[23] T. J. Lee, J. E. Rice, G. E. Scuseria, H. F. Schaefer III, Theoretical investigations of molecules composed only of fluorine, oxygen and nitrogen: determination of the equilibrium structures of FOOF, (NO)2 and FNNF and the transition state structure for FNNF cis-trans isomerization, *Theor. Chim. Acta* 75 (1989) 81–98.

[24] C. Lee, W. Yang, R. G. Parr, *Phys. Rev. B* Development of the Colle-Salvetti correlation-energy formula into a functional of the electron density, 37 (1988) 785–789.

[25] A. D. Becke, Density functional – thermochemistry. III. The role of exact exchange, *J. Chem. Phys.* 98 (1993) 5648.

[26] P. J. Stephens, F. J. Devlin, C. F. Chabalowski, M. J. Frisch, Ab Initio Calculation of Vibrational Absorption and Circular Dichroism Spectra Using Density Functional Force Fields, *J. Phys. Chem.* 98 (1994) 11623.

[27] R. Krishnan, J. S. Binkley, R. Seeger, J. A. Pople, Self-consistent molecular orbital methods. XX. A basis set for correlated wave functions, *J. Chem. Phys.* 72 (1980) 650.

[28] C. Gonzalez, H. B. Schlegel, An improved algorithm for reaction path following, *J. Chem. Phys.* 90 (1989) 2154.

[29] C. Gonzalez, H. B. Schlegel, Reaction path following in mass-weighted internal coordinates, *J. Phys. Chem.* 94 (1990) 5523–5527.

[30] S. Lakshmanan, R. F. K. Spada, F. B. C. Machado, W. L. Hase, Potential Energy Curves for Formation of the CH_2O_2 Criegee Intermediate on the $^3CH_2 + {}^3O_2$ Singlet and Triplet Potential Energy Surfaces, *J. Phys. Chem. A* 123 (2019) 8968–8975.

[31] J. A. Montgomery, M. J. Frisch, J. W. Ochterski, G. A. Petersson, *J. Chem. Phys.* 110 (1999) 2822.

[32] J. P. Wagner, Gauging stability and reactivity of carbonyl O-oxide Criegee intermediates, *Phys. Chem. Chem. Phys.* 21 (2019) 21530– 21540.

[33] P. Aplincourt, M. F. Ruiz-López, Theoretical Investigation of Reaction Mechanisms for Carboxylic Acid Formation in the Atmosphere, *J. Am. Chem. Soc.* 122 (2000) 8990–8997.

[34] P. Xiao, J.-J. Yang, W.-H. Fang, G. Cui, QM/MM studies on ozonolysis of α-humulene and Criegee reactions with acids and water at air-water/acetonitrile interfaces, *Phys. Chem. Chem. Phys.* 20 (2018) 16138–16150.

[35] M. Kumar, D. H. Busch, B. Subramaniam, W. H. Thompson, Role of Tunable Acid Catalysis in Decomposition of α-Hydroxyalkyl Hydroperoxides and Mechanistic Implications for Tropospheric Chemistry, *J. Phys. Chem. A* 118 (2014) 9701–9711.

[36] M. A. H. Khan, K. Lyons, R. Chhantyal-Pun, M. R. McGillen, R. L. Caravan, C. A. Taatjes, A. J. Orr-Ewing, C. J. Percival, D. E. Shallcross, Investigating the Tropospheric Chemistry of Acetic Acid Using the Global 3-D Chemistry Transport Model, STOCHEM-CRI, *J. Geophys Res. Atmos* 123 (2018) 6267–6281.

[37] T. Banu, K. Sen, A. K. Das, Atmospheric Fate of Criegee Intermediate Formed During Ozonolysis of Styrene in the Presence of H_2O and NH_3: The Crucial Role of Stereochemistry, *J. Phys. Chem. A* 122 (2018) 8377–8389.

[38] M. Kumar, D. H. Busch, B. Subramaniam, W. H. Thompson, Barrierless tautomerization of Criegee intermediates via acid catalysis. *Phys. Chem. Chem. Phys.* 16 (2014) 22968–22973.

[39] A. Novelli, L. Vereecken, J. Lelieveld, H. Harder, Direct observation of OH formation from stabilised Criegee intermediates, *Phys. Chem. Chem. Phys.* 16 (2014) 19941– 19951.

[40] L. Vereecken, D. R. Glowacki, M. J. Pilling, Theoretical chemical kinetics in tropospheric chemistry: Methodologies and applications. *Chem. Rev.* 115 (2015) 4063–4114.

[41] F. Sarrami, F. Mackenzie-Rae, A. Karton, A computational investigation of the sulphuric acid-catalysed 1,4-hydrogen transfer in higher Criegee intermediates. *Int. J. Quantum Chem.* 118 (2018) e25599.

[42] L. Vereecken, J. S. Francisco, Theoretical studies of atmospheric reaction mechanisms in the troposphere, *Chem. Soc. Rev.* 41 (2012) 6259–6293.

[43] R. J. Buszek, J. S. Francisco, J. M. Anglada, Water effects on atmospheric reactions, *Int. Rev. Phys. Chem.* 30 (2011) 335.

[44] V. Vaida, Perspective: water cluster mediated atmospheric chemistry*, J. Chem. Phys.* 135 (2011) 020901.

[45] E. Vohringer-Martinez, B. Hansmann, H. Hernandez, J. S. Francisco, J. Troe, B. Abel, Water Catalysis of a Radical-Molecule Gas-Phase Reaction, *Science* 315 (2007) 497–501.

[46] A. Karton, Inorganic acid-catalyzed tautomerization of vinyl alcohol to acetaldehyde. *Chem. Phys. Lett.* 592 (2014) 330–333.

[47] H. Xie, W. Jiang, Y. Xue, Z. Hou, Y. Wang, D. Wu, T. Liu, J. Wang, L. Tang, Effect of water on carbonation of mineral aerosol surface models of kaolinite: a density functional theory study, *Environ. Earth Sci.* 73 (2015) 7053.

[48] D. Cremer, E. Kraka, P. G. Szalay, Decomposition modes of dioxirane, methyldioxirane and dimethyldioxirane — a CCSD(T), MR-AQCC and DFT investigation, *Chem. Phys. Lett.* 292 (1998) 97–109.